



THE UNIVERSITY *of* EDINBURGH

## Edinburgh Research Explorer

### **Comparison of amine-impregnated mesoporous carbon with microporous activated carbon and 13X zeolite for biogas purification**

**Citation for published version:**

Gibson, JJA, Gromov, A, Brandani, S & Campbell, EEB 2017, 'Comparison of amine-impregnated mesoporous carbon with microporous activated carbon and 13X zeolite for biogas purification', *Journal of Porous Materials*, vol. 24, no. 6, pp. 1473-1479. <https://doi.org/10.1007/s10934-017-0387-0>

**Digital Object Identifier (DOI):**

[10.1007/s10934-017-0387-0](https://doi.org/10.1007/s10934-017-0387-0)

**Link:**

[Link to publication record in Edinburgh Research Explorer](#)

**Document Version:**

Peer reviewed version

**Published In:**

Journal of Porous Materials

**General rights**

Copyright for the publications made accessible via the Edinburgh Research Explorer is retained by the author(s) and / or other copyright owners and it is a condition of accessing these publications that users recognise and abide by the legal requirements associated with these rights.

**Take down policy**

The University of Edinburgh has made every reasonable effort to ensure that Edinburgh Research Explorer content complies with UK legislation. If you believe that the public display of this file breaches copyright please contact [openaccess@ed.ac.uk](mailto:openaccess@ed.ac.uk) providing details, and we will remove access to the work immediately and investigate your claim.



# **Comparison of amine-impregnated mesoporous carbon with microporous activated carbon and 13X zeolite for biogas purification**

J. A. A. Gibson,<sup>a</sup> A. V. Gromov,<sup>b</sup> S. Brandani<sup>a</sup> and E.E.B. Campbell<sup>b,c,†</sup>

a: School of Engineering, University of Edinburgh, Edinburgh EH9 3FB, U.K.

b: EaStCHEM and School of Chemistry, University of Edinburgh, Edinburgh EH9 3FJ, U.K.

c: Division of Quantum Phases and Devices, School of Physics, Konkuk University, Seoul 143-701, Korea

†:Corresponding author, Eleanor.campbell@ed.ac.uk

## **Abstract**

Three materials are directly compared for their potential for biogas purification: 13X zeolite, microporous activated carbon and mesoporous activated carbon impregnated with polyethyleneimine. The amine-impregnated material shows the highest selectivity for CO<sub>2</sub> over CH<sub>4</sub> but this should be balanced by the higher operating temperature required. All three materials could be used for biogas purification with the advantages and disadvantages clearly presented.

**Keywords:** porous carbon, CO<sub>2</sub>, impregnation, adsorption, biogas

## 1. Introduction

With the world's ever increasing requirement for green energy, there is great potential to reduce carbon emissions through the optimisation of current energy generation methods. One such green technology is the production of biogas via the fermentation of plant material or waste to produce a mixture of predominantly CO<sub>2</sub> and CH<sub>4</sub>.

Depending on the process used during production, along with the type of fermented material, the composition of the produced gas can vary significantly. However, from an anaerobic digester, a significant portion of the produced gas will always be CO<sub>2</sub>.

In order to enhance the gas stream for energy production processes, an adsorption process can be used to purify the individual components.[1] Purification of the gas mixtures to produce two high purity gas streams has the added benefit of producing a higher value product of close to pure methane along with a CO<sub>2</sub> stream that could potentially be sequestered, preventing the release of CO<sub>2</sub> into the atmosphere and hence reducing the environmental impact of the process. This is referred to as biogas upgrading and, as a result of its green power generation credentials, the optimisation of the upgrading process has recently begun to attract interest as an area of research.[1-3] The optimal technology for biogas upgrading is highly dependent on the specific biogas process/plant. The biogas feedstock, the scale of the plant and the acceptable concentration of impurities in the product streams are all important factors in selecting an upgrading technology. A variety of technologies have been investigated and, in certain cases, implemented such as water scrubbing and pressure swing adsorption (PSA) [4], cryogenic separation, chemical absorption, physical absorption and membrane separation [5, 6]. A review comparing the cost and investigating the appropriate utilisation of the various approaches was recently published by Sun et al. [7]. From this review it is clear that further work is required to

establish the potential of the different technologies if biogas upgrading is to find more widespread application. There are also several recent reports that propose systems to lower the cost of gas separation. In 2015 Kim et al. [8] proposed a four column PSA process using a carbon molecular sieve as adsorbent that only had a selectivity for CO<sub>2</sub> over CH<sub>4</sub> of 1.9. Grande et al. proposed a layered pressure swing adsorption system where a kinetic adsorbent such as a carbon molecular sieve was layered with an equilibrium adsorbent [9]. This combination improved the productivity of the set-up and resulted in a potential size reduction of the separation unit by up to 60%. The selection of an appropriate, novel adsorbent could significantly enhance the efficiency of an adsorption separation process. However, there are only few reports in the literature regarding the development of optimised adsorbent material for biogas upgrading.

The main materials used in PSA are zeolites and activated carbons. Alonso-Vicario et al. compared commercial zeolites 13X, 5A and natural clinoptilolite using breakthrough experiments and concluded that despite its lower CO<sub>2</sub> capacity, clinoptilolite was preferred as it was able to separate both the CO<sub>2</sub> and H<sub>2</sub>S that was present in their biogas stream, from CH<sub>4</sub> [10]. Various activated carbons have been investigated for their ability to separate CO<sub>2</sub> from CH<sub>4</sub> with a selectivity of 2-4, depending on the material and the process conditions [10, 11]. Triamine grafted pore expanded silica was investigated by Belmabkhout et al. who proposed, on the basis of single component adsorption data, that it had great potential to separate acidic gases from CH<sub>4</sub> with high selectivity [12].

In this paper, we compare the selectivity for CO<sub>2</sub> over CH<sub>4</sub> of three different adsorbents: commercial zeolite (13X), commercial microporous activated carbon (micro-AC) and an amine-impregnated activated carbon (meso-AC2-PEI). The first

two materials provide a benchmark and direct comparison between well-characterised and studied materials while the third material is, to our knowledge, the first report of the study of an amine-impregnated activated carbon for biogas upgrading. The three materials allow a direct comparison of the advantages and disadvantages of using physical adsorption (13X, micro-AC) or chemical adsorption (meso-AC-PEI) to separate CO<sub>2</sub> from CH<sub>4</sub>. We show that the impregnated AC material has the highest selectivity ( $\rightarrow \infty$ ) that, together with its insensitivity to water but relatively high operating temperature, could make this a very suitable class of material for integration into temperature swing adsorption processes.

## **2. Experimental Methods**

### **2.1 Materials**

The zeolite 13X and the microporous activated carbon (SRD 10061) are commercially available materials from UOP (Honeywell) and Calgon Carbon, respectively. The microporous-AC had a BET surface area of 1336 m<sup>2</sup> g<sup>-1</sup> with a total pore volume of 0.68 cm<sup>3</sup> g<sup>-1</sup> of which 0.59 cm<sup>3</sup> g<sup>-1</sup> consisted of micro-pores with dimensions < 2nm [13]. The meso-porous-AC material was synthesised by a templating method using sucrose and a silicagel with an average pore size of 150 Å, following the procedure described previously [13]. It had a BET surface area of 1254 m<sup>2</sup> g<sup>-1</sup> and a total pore volume of 3.1 cm<sup>3</sup> g<sup>-1</sup>. In this case, ~2.9 cm<sup>3</sup> g<sup>-1</sup> consisted of meso-pores with dimensions in the range 2nm – 50 nm (the pore size distribution is provided in the Electronic Supplementary Information). As published previously, impregnation of mesoporous-AC with amines was shown to significantly increase the CO<sub>2</sub> uptake capacity at 0.1 bar, changing the mechanism from physisorption on the empty material to chemisorption on the impregnated material [13]. Large molecular weight

amines were found to be more suitable due to their higher thermal stability and recyclability in spite of the slightly less efficient use of the amino groups.

Microporous-AC was shown to be unsuitable for impregnation due to the tendency for pore blocking. In the present study, the mesoporous AC was impregnated with polyethyleneimine (PEI, MW 1200) at a ratio of ca. two parts polymer to one part carbon, meso-AC-PEI (65.7 wt.%, corresponding to approximately  $\frac{3}{4}$  pore filling), following the procedure detailed previously [13].

## **2.2 Extended Zero-Length Column Breakthrough Technique**

The extended zero-length column technique (E-ZLC) is similar to the more traditional ZLC which is a powerful method for providing an initial ranking of adsorbents, requiring only small amounts of sample (5 – 15 mg) [14]. The E-ZLC makes use of a larger column, ca. three times the length of the ZLC, housed in a 1/8" Swagelok bulkhead connector. This allows more sample to be packed in the adsorption column to achieve a clear separation of components in a binary mixture and determine the binary adsorption selectivity [15]. The advantage of E-ZLC over a traditional breakthrough column is that a relatively small amount of sample is required (ca. 50 mg, compared to ca. 5 g for a standard column) and that the column can be considered to be isothermal, as experimentally tested and discussed previously [15]. In a typical experiment, the sample is packed in the column and regenerated at high temperature under inert gas flow. The sample is cooled to the temperature of interest and then equilibrated with a gas stream containing a known partial pressure of sorbates, in the present case 45% CO<sub>2</sub>, 55% CH<sub>4</sub>. The gas stream is then switched to a stream of pure purge gas (N<sub>2</sub>) and the desorption profile is monitored by a mass spectrometer.

Three E-ZLC were packed with the commercial zeolite 13X (63.8 mg), the micro-AC (37.9 mg) and the meso-AC-PEI (25.2 mg). The different masses used for the experiments are a consequence of the different densities of the adsorbents. The breakthrough experiments were run at 35°C for 13X and micro-AC, which as physisorbents have a higher CO<sub>2</sub> capacity at lower working temperatures, and at 75 °C for meso-AC-PEI, due to the slower reaction kinetics of the impregnated chemisorption material [13]. The desorption profiles were determined for different gas flow rates and modelled using the Cysim simulator [15, 16].

The simulation parameters needed to reproduce the experimental breakthrough response of all three samples are reported in Table 1. Comparison with experimentally determined volumetric isotherms, measured with an iQ1 volumetric system (Quantachrome), was used to determine the parameters used in the simulations for 13X and micro-AC.

### **3. Results and Discussion**

#### **3.1. Volumetric Isotherms**

The volumetric isotherms measured for 13X and micro-AC and fitted to obtain the Langmuir isotherm parameters used in the breakthrough simulations are shown in Figures 1 and 2 for CO<sub>2</sub> and N<sub>2</sub> adsorption experiments. The lines show the best fits with the extracted parameters tabulated in Table 1.

Table 1: Isotherm parameters used in the Cysim simulations.  $q_s$ : saturation capacity,  $b_0$ :

		$q_{s1}$ (mmol g <sup>-1</sup> )	$q_{s2}$ (mmol g <sup>-1</sup> )	$b_{1,0}$ (bar <sup>-1</sup> )	$b_{2,0}$ (bar <sup>-1</sup> )	$\Delta H_1$ (J mol <sup>-1</sup> )	$\Delta H_2$ (J mol <sup>-1</sup> )
13X	CO <sub>2</sub>	2.08	3.03	$3.52 \times 10^{-6}$	$1.32 \times 10^{-6}$	45793	37988
	N <sub>2</sub>	2.08	3.03	$2.90 \times 10^{-7}$	$2.90 \times 10^{-7}$	30555	30555
	CH <sub>4</sub>	2.08	3.03	$2.20 \times 10^{-3}$	$2.20 \times 10^{-3}$	10000	10000
Micro-AC	CO <sub>2</sub>	4.9		$2.17 \times 10^{-5}$		27000	
	N <sub>2</sub>	4.9		$4.92 \times 10^{-6}$		23940	
	CH <sub>4</sub>	4.9		$3.50 \times 10^{-4}$		17000	
Meso-AC- PEI	CO <sub>2</sub>	1.74		$3.00 \times 10^{-11}$		88000	
	N <sub>2</sub>						
	CH <sub>4</sub>	1.74		$1.00 \times 10^{-2}$		1450	

equilibrium rate constant,  $\Delta H$ : heat of adsorption.

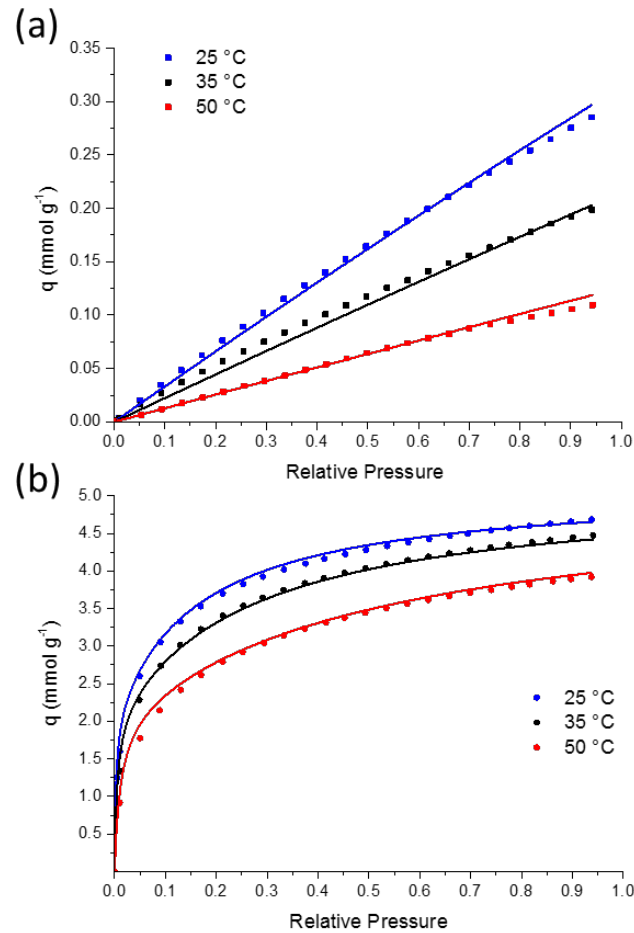


Fig. 1. Volumetric isotherms measured for 4mm pellets of 13X at three different temperatures, 25 °C, 35 °C and 50 °C along with a dual-site Langmuir fit. Langmuir fit



parameters given in Table 1. (a) N<sub>2</sub>, (b) CO<sub>2</sub>. Relative pressure =  $P/P_0$  where  $P_0 = 760$  torr  
Adapted from SI in ref. [15].

Volumetric isotherms could not be measured for meso-AC-PEI since the amine could potentially damage the iQ1 system. In this case the simulation parameters were solely established by fitting the E-ZLC breakthrough curves.

A dual-site Langmuir isotherm was used to fit the 13X data with the same saturation capacity ( $q_s$ ) used for each gas on each site, to ensure thermodynamic consistency. A single-site Langmuir expression was used to fit the micro-AC sample, and also assumed for the breakthrough measurements on the meso-AC-PEI sample.

### 3.2. E-ZLC Breakthrough Measurements

The adsorption breakthrough profiles of 13X, micro-AC and meso-AC-PEI are shown in Fig. 3. Time 0 indicates the change from the pure purge gas (N<sub>2</sub>) to the mixture of 45% CO<sub>2</sub> and 55% CH<sub>4</sub>. A clear separation of the CO<sub>2</sub> and CH<sub>4</sub> is seen for the 13X sample, Fig. 3(a). At a flow rate of 10 cm<sup>3</sup> min<sup>-1</sup> the breakthrough times are approximately 9 s and 84 s for CH<sub>4</sub> and CO<sub>2</sub>, respectively, after subtraction of the breakthrough time of the blank response (14 s). “Roll-up” of the CH<sub>4</sub> ( $C/C_0 > 1$ ) is observed. This is due to all the CO<sub>2</sub> being adsorbed by the 13X, with the consequence that the gas at the outlet, prior to the breakthrough of CO<sub>2</sub> is pure CH<sub>4</sub>. The magnitude of the roll-up is larger than expected due to the over-response of the mass spectrometer to the large step change in the gas phase concentration of CH<sub>4</sub> as it breaks through.

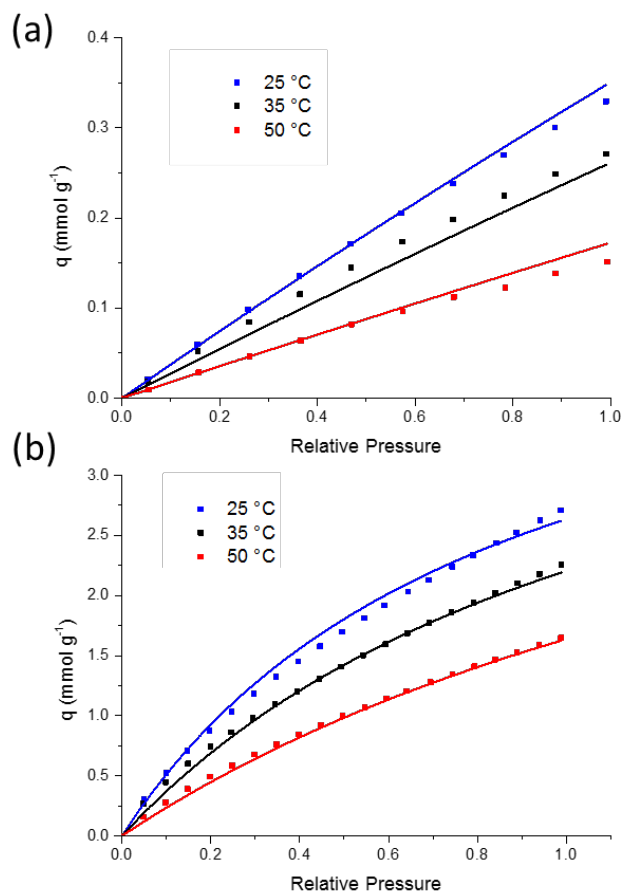


Fig. 2. Volumetric isotherms measured for micro-AC granules at three different temperatures, 25 °C, 35 °C and 50 °C along with a single-site Langmuir fit. Langmuir fit parameters given in Table 1. (a) N<sub>2</sub> (b) CO<sub>2</sub> Relative pressure =  $P/P_0$  where  $P_0 = 760$  torr.

The results for micro-AC and meso-AC-PEI can be seen in Figs. 3(b) and (c). In both materials the CH<sub>4</sub> and CO<sub>2</sub> breakthrough at different times and the materials can therefore be used to separate the two gases. However, a more detailed analysis is required to compare the materials and assess the selectivity of CO<sub>2</sub> over CH<sub>4</sub>. In order to avoid the intensity artefacts from the mass spectrometer signal in the adsorption measurements, it is more convenient and reliable to compare the

performance of the materials in the desorption branch. In this case there are no artefacts due to the performance of the mass spectrometer and the desorption of the two gases from the saturated beds was evaluated for several different flow rates of the pure N<sub>2</sub> purge gas (Figs. 4 and 5). By calculating the adsorbed amount from the desorption experiment the equilibrium adsorbed amount of each component can be evaluated accurately. However, if the adsorption experiments are analysed by first moment analysis, then care must be taken not to over-estimate the adsorbed amount of the weakly adsorbed component (CH<sub>4</sub>). A significant amount of the weakly adsorbed component will be initially adsorbed and then desorbed as the concentration front of the strongly adsorbed component (CO<sub>2</sub>) breaks through the adsorption bed. The binary selectivity for each material was evaluated by fitting the experimental data with the Cysim simulator, where possible using the parameters that had been obtained independently from the volumetric isotherms. As there was a large step change in the concentration of the gases the flow rate passing the detector is not constant in time. Several methods have been suggested to correct for the flow rate but generally are only valid for small step changes [17]. The Cysim simulation corrects for the flow rate and ensures that the mass balance closes [16]. By calculating the selectivity from the desorption curves, the true binary selectivity is established because the integration of the area under the curve (accounting for the variable flowrate) directly yields the adsorbed amount of the binary mixture.

The desorption curves for 13X are shown in Fig. 4 along with the model prediction on a semi-log plot vs. time. The parameters determined by the volumetric isotherm measurements, were used to simulate the CO<sub>2</sub> desorption curves and the methane parameters were carefully fitted to match the experimental data. The adsorbed

amounts of each component, extracted from the simulations are provided in Table 2 along with the selectivity of the adsorbents with respect to CO<sub>2</sub>, defined as

$$S_{ADS} = \frac{q_{CO_2}/q_{CH_4}}{P_{CO_2}/P_{CH_4}} \quad (1)$$

where  $P_{CO_2} = 0.45$  bar and  $P_{CH_4} = 0.55$  bar.

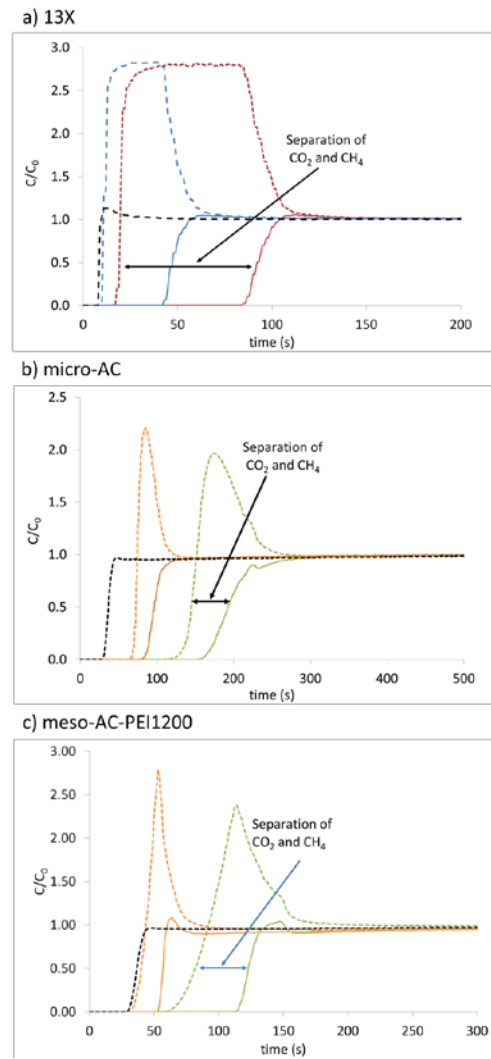


Fig. 3. E-ZLC concentration profiles during the adsorption step as a function of time (a) 13X, 35 °C , 61.3 mg (b) micro-AC, 35 °C, 37.9 mg (c) meso-AC-PEI, 75 °C, 25.2 mg. Multiple flow rates (green: 1 cm<sup>3</sup> min<sup>-1</sup>, orange: 2.5 cm<sup>3</sup> min<sup>-1</sup>, , red: 10 cm<sup>3</sup> min<sup>-1</sup> blue: 20 cm<sup>3</sup> min<sup>-1</sup>, black: blank response a) 10 cm<sup>3</sup> min<sup>-1</sup>, b,c) 2.5 cm<sup>3</sup> min<sup>-1</sup>. Full line: CO<sub>2</sub>, dashed line; CH<sub>4</sub>.

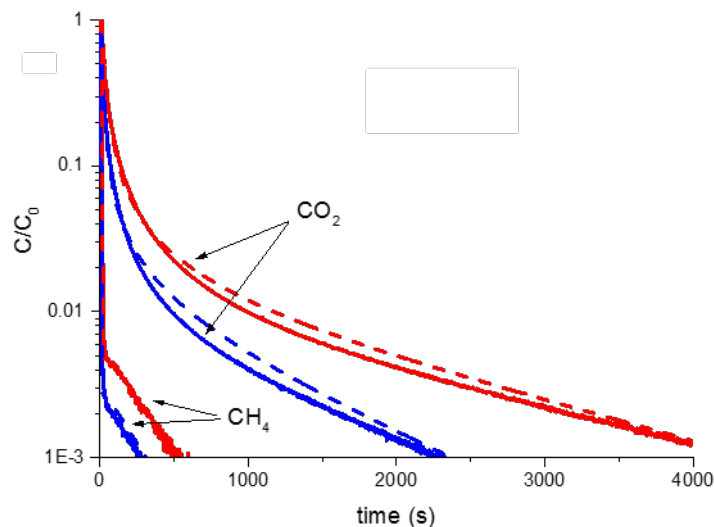


Fig.4. 13X desorption breakthrough curves for two purge gas flow rates plotted vs. time on a semi-log plot together with simulation results using parameters extracted from volumetric isotherm measurements (Fig. 1) Experimental data: solid lines, simulation: dashed lines. blue:  $20 \text{ cm}^3 \text{ min}^{-1}$ . red:  $10 \text{ cm}^3 \text{ min}^{-1}$

The experimental breakthrough desorption curves for all three materials, plotted on a linear scale together with the Cysim simulations are shown in Fig. 5. A clear separation of the components was seen for each sample with a significantly higher quantity of  $\text{CO}_2$  than  $\text{CH}_4$  adsorbed at equilibrium in each case. In the case of 13X and meso-AC-PEI, virtually no  $\text{CH}_4$  was adsorbed by the adsorbent at equilibrium. In the inset of Fig. 5(a) and the main body of Fig 5(c) the concentration profile of the  $\text{CH}_4$  from the adsorption bed practically overlaps the system's blank run response. The total uptake of  $\text{CO}_2$  was less for the impregnated sample than for 13X, Table 2, however, the presence of water does not significantly hinder the uptake of  $\text{CO}_2$  by amine-impregnated samples [18, 19], unlike the situation for 13X [20]. This is

advantageous as biogas often has a high water content. The meso-AC-PEI adsorbs more CO<sub>2</sub> per unit mass than the micro-AC. CO<sub>2</sub> binds strongly to the amine, as can be seen from the shape of the desorption curve and also from the high value extracted for the heat of adsorption,  $\Delta H$ , of approximately 90 kJ mol<sup>-1</sup>, Table 1. The CO<sub>2</sub> is therefore very favourably adsorbed compared to the CH<sub>4</sub> and the majority of the CO<sub>2</sub> starts to desorb from the sample at a lower CO<sub>2</sub> partial pressure (low  $C/C_0$ ) than is the case for 13X and meso-AC. The strong chemisorption between the amine and the CO<sub>2</sub> provides high selectivity at low partial pressure.

Table 2: Adsorption of CO<sub>2</sub> and CH<sub>4</sub> from biogas gas stream (45% CO<sub>2</sub>, 55% CH<sub>4</sub>) and calculated selectivity for CO<sub>2</sub>. Simulation parameters used to extract the values are provided in Table 1. Values in brackets for micro-AC correspond to the selectivities and adsorbed amounts as calculated from cysim simulation using adjusted parameters to obtain the best fit to the experimental data as shown in the Supplementary Material (Fig. 3).

	13X	Micro-AC	Meso-AC- PEI
$q_{CO_2}$ (mmol g <sup>-1</sup> )	3.83	1.14 (1.02)	1.73
$q_{CH_4}$ (mmol g <sup>-1</sup> )	0.07	0.46 (0.48)	0.00
Selectivity, $S_{ADS}$	66	3.0 (2.59)	$\rightarrow \infty$

As expected, the selectivity of 13X is greater than micro-AC due to the strong interactions between the CO<sub>2</sub> quadrupole and the zeolite surface. Under equilibrium conditions, very little CH<sub>4</sub> was adsorbed by the zeolite and no detectable CH<sub>4</sub>

adsorption was recorded for the meso-AC-PEI material. An accurate fitting of the system blank response and the sample data is required to extract an accurate value for the amount of CH<sub>4</sub> that has been adsorbed. The blank response of the system was fitted with Cysim prior to the sample fitting. The blank response curves at each flow rate along with their associated fit can be found in the Supplementary Material. The methane concentration profile for meso-AC-PEI was so close to the system response that the selectivity tended towards infinity. Both 13X and meso-AC-PEI are thus highly selective towards CO<sub>2</sub> over CH<sub>4</sub>. Silva et al. reported the experimental selectivity of 13X to range from 37 at low pressure (0.67 atm) and low temperature (313 K) to 5 at high temperature (423 K), which is of the same order of magnitude although significantly lower than the experimental selectivity of 66 reported here, possibly a consequence of trace amounts of water in the earlier measurements [21]. A comparison of the impregnated meso-AC and the micro-AC shows that the impregnation significantly enhanced the selectivity of the carbon material. The selectivity of micro-AC is limited since, unlike the other two materials, the micro-AC adsorbs a significant amount of CH<sub>4</sub> as well as CO<sub>2</sub>. The simulated curves for micro-AC, based on the pure component isotherms (Table 1) as seen in Fig 5b were not perfect due to non-ideal adsorption behaviour. Therefore for this case the CO<sub>2</sub> isotherm parameters were also adjusted to simulate more closely the experimental data (as shown in Supplementary Material Figure 3). This allowed the selectivity corresponding to the best fit to the experimental data to be reported taking into account any necessary flow rate corrections. To achieve the best fit, the  $b_{1,0}$  parameter for CO<sub>2</sub> was adjusted from  $2.17 \times 10^{-5} \text{ bar}^{-1}$  to  $1.87 \times 10^{-5} \text{ bar}^{-1}$ . Gil et al. [11] reported a selectivity factor of 3.2 for CO<sub>2</sub> over CH<sub>4</sub> on a comparable microporous activated carbon, in good agreement with the selectivity of 3.0 (2.59) reported here.

Although the unmodified activated carbons may have a disadvantage over zeolites in terms of selectivity, activated carbons are relatively inexpensive and stable over many cycles. As shown here, the selectivity can be significantly enhanced by modifying the adsorbent through impregnation with polyamine. The basic amine groups preferentially chemisorb the  $\text{CO}_2$  and, additionally, loading the pores with amine through a wet impregnation method has the added benefit of filling the pore volume of the activated carbon, greatly reducing the number of sites available for physisorption of  $\text{CH}_4$ . To facilitate the chemisorption and increase the reaction kinetics the process must be carried out at elevated temperature, again reducing the volume of adsorbed  $\text{CH}_4$  and further enhancing the selectivity of the impregnated activated carbon.

## **Conclusions**

All three investigated materials in this study, 13X, micro-AC and meso-AC-PEI, can be used to separate  $\text{CO}_2$  from  $\text{CH}_4$  in a biogas upgrading adsorption process. Both meso-AC-PEI and 13X have high selectivity, adsorbing only small (in the case of meso-AC-PEI undetectable) amounts of  $\text{CH}_4$ . Depending on the type of process to be developed, the biogas feedstock and the purity requirements of the product streams, all three adsorbents could potentially be utilized to upgrade biogas.

Commercial zeolite 13X has a high selectivity of up to 66, however, in the presence of water vapour, the total uptake of  $\text{CO}_2$  is significantly reduced [20] and it would therefore be desirable to ensure dry feed gas.

The required operation temperature for the highly selective amine-impregnated material would make it suitable for integration into a temperature swing adsorption process, using excess heat from the biogas plant for regeneration. However, due to the



high input partial pressure of CO<sub>2</sub>, it may not always be necessary to incorporate the strong amine-CO<sub>2</sub> chemisorption sites. In some cases, the high regeneration costs may outweigh the advantages of the high selectivity of the amine impregnated material. Process simulations would be required in each case to fully assess the suitability and viability of each material.

As a larger number of biogas plants are introduced to the energy mix, novel materials will be required to upgrade the fuel to the required purity in the most economical manner possible. It is likely that no single material will be suitable for all situations and it is therefore important to understand the parameters influencing the performance and directly compare different classes of material.

## **Acknowledgements**

This work has been performed with financial support from the EPSRC AMPGas project EP/J0277X/1. We thank Rachel Rayne for initial work on the preparation of the meso-AC material. EC thanks JSPS and the University of Nagoya for support and hospitality while this manuscript was being written.

Raw data for the volumetric isotherms and breakthrough curves is available at <http://hdl.handle.net/10283/2335>

Supplementary Material is available.

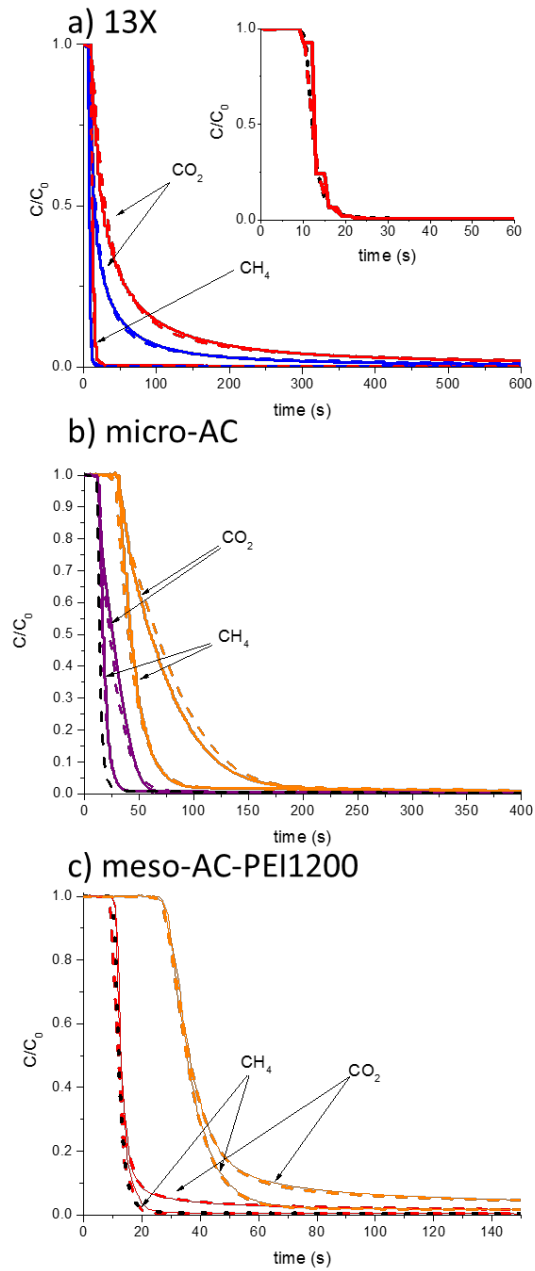


Fig. 5. Experimental breakthrough desorption curves for selected  $N_2$  flow rates along with Cysim simulations. (a) 13X, 35 °C, 63.8 mg (b) micro-AC, 35 °C, 37.9 mg (c) meso-AC-PEI, 75 °C, 25.2 mg. Dashed lines: simulations. Solid lines: experimental concentration profiles. Multiple flow rates (green: 1  $\text{cm}^3 \text{min}^{-1}$ , orange: 2.5  $\text{cm}^3 \text{min}^{-1}$ , purple: 7.5  $\text{cm}^3 \text{min}^{-1}$ , red: 10  $\text{cm}^3 \text{min}^{-1}$ , blue: 20  $\text{cm}^3 \text{min}^{-1}$  black: blank response 10  $\text{cm}^3 \text{min}^{-1}$ . Black dots show blank response at a),c) 10  $\text{cm}^3 \text{min}^{-1}$  b) 7.5  $\text{cm}^3 \text{min}^{-1}$  .

## References

1. Wu B, Zhang X, Xu Y, Bao D, Zhang S. 2015. J Clean Prod. **101**: 251-61.
2. Bacsik Z, Cheung O, Vasiliev P, Hedin N. 2016. Appl Energ. **162**: 613-21.
3. Niesner J, Jecha D, Stehlik P. 2013. Chem Eng Trans. **35**: 517-22.
4. Yin C, Sun W, Yang H, Zhang D. 2015. Chem Eng Sci. **91**: 732-41.
5. Ozturk B, Demirciyeva F. 2013. Chem Eng J. **222**: 209-17.
6. Scholz M, Alders M, Lohaus T, Wessling M. 2015. J Membrane Sci. **474**: 1-10.
7. Sun Q, Li H, Yan J, Liu L, Yu Z, Yu X. 2015. Renew Sust Energ Rev. **51**: 521-32.
8. Kim YJ, Nam YS, Kang YT. 2015. Energy. **91**: 732-41.
9. Grande CA, Rodrigues AE. 2007. Ind Chem Eng Res. **46**: 7844-8.
10. Alonso-Vicario A, Ochoa-Gomez JR, Gil-Rio S, Gomez-Jimenez-Aberasturi O, Rairez-Lopez CA, Torrecilla-Soria J, et al. 2010. Micropor & Mesopor Mat. **134**: 100-7.
11. Gil MV, Alvarez-Gutierrez N, Martinez M, Rubiera F, Pevida C, Moran A. 2015. Chem Eng J. **269**: 148-58.
12. Belmabkhout Y, De Weireld G, Sayari A. 2009. Langmuir. **25**: 13275-8.
13. Gibson JAA, Gromov AV, Brandani S, Campbell EEB. 2015. Micropor & Mesopor Mat. **208**: 129-39.
14. Xu H, Brandani S, Benin AI, Willis RR. 2015. Ind Eng Chem Res. **54**: 6772-80.

15. Gibson JAA, Mangano E, Shiko E, Greenaway AG, Gromov AV, Lozinska MM, et al. 2016. Ind EngChem Res. **55**: 3840-51.
16. Friedrich D, Ferrari MC, Brandani S. 2013. Ind Eng Chem Res. **52**: 8897-905.
17. Wang H, Brandani S, Lin G, Hu X. 2011. Adsorption. **17**: 687-94.
18. Subagyono DJN, M. M, Knowles GP, Chaffee AL. 2014. Micropor Mesopor Mat. **186**: 84-93.
19. Sayari A, Belmabkhout Y. 2010. J Am Chem Soc. **132**: 6312-4.
20. Brandani F, Ruthven DM. 2004; Ind Engi Chem Res. **43**: 8339-44.
21. Silva JAC, Cunha AF, Schumann K, Rodrigues AE. 2014. Micropor Mesopor Mat. **187**: 100-7.